Characteristics of Halo Current in JT-60U

Y. Neyatani, Y. Nakamura, R. Yoshino, T. Hatae and the JT-60 team

Naka Fusion Research Establishment, Japan Atomic Energy Research Institute
Mukoyama 801-1, Naka-mach, Naka-gun, Ibaraki-ken, 311-01, Japan

ABSTRACT

Halo currents and their toroidal peaking factor (TPF) have been measured in JT-60U by Rogowski coil type halo current sensors. The electron temperature in the halo region was around 10 eV at 1 ms before the timing of the maximum halo current. The maximum $TPF*I_h/I_{p0}$ was 0.52 in the operational range of $I_p = 0.7 \sim 1.8$ MA, $B_T = 2.2 \sim 3.5$ T, including ITER design parameters of $\kappa > 1.6$ and $q_{95} = 3$, which was lower than that of the maximum value of ITER data base (0.75). The magnitude of halo currents tended to decrease with the increase in stored energy just before the energy quench and with the line integrated electron density at the time of the maximum halo current. A termination technique in which the current channel remains stationary was useful to avoid halo current generation. Intense neon gas puffing during the VDE was effective for reducing the halo currents.

1. INTRODUCTION

A current flowing directly into a vacuum vessel from a plasma (called halo current) is observed during disruptions in tokamaks. This halo current will produce an intense electromagnetic force on the in-vessel components in ITER, such as the blanket module and the divertor cassette. Therefore, the halo current is one of the critical issues. The design value for ITER is mainly determined from the data base from medium and small size tokamaks [1]. Further investigation on the characteristics of the halo current in large tokamaks is urgently required. Its parameter dependence must be established, and mitigation and/or avoidance methods applicable to ITER must be developed. In JT-60U, sensors for the halo current (Rogowski coils) were newly installed during the divertor modification in May 1997, enabling the measurement of its toroidal and poloidal distribution.

2. EXPERIMENTAL RESULTS

2.1 Plasma behavior during simulated VDE

For the halo current study, the most dangerous disruption caused by vertical displacement event (VDE) was experimentally simulated, in which a plasma was actively controlled to move downward (Fig. 1). In this case, a halo current flows into the inside baffle plate and back to the plasma through the outside baffle plate, as was expected. When the plasma attaches the baffle plate, total D_α signal measured at the plasma attached position increases. After that, an energy quench occurs with a strong D_α and dB/dt bursts (13.0372 s in Fig. 2). D_α emissions from the corners of inside baffle, dome and outside baffle plate are caused by an energy release from a plasma core (Fig. 2(b)). When q_s becomes close to unity (13.0437 s in Fig. 2), D_α and dB/dt bursts occurred again. Magnitude of dB/dt (n=0) jumps at the similar time scale of the energy quench within 40 micro seconds. In this burst, only a D_α emission at the plasma central channel increases (Fig. 2(c)). Just after the burst at $q_s \sim 1$, a halo current rapidly increases and reaches to its maximum. The maximum halo current is more than 80 % of the plasma current in this case. In some cases, no burst at $q_s \sim 1$ was observed since q_s at the time of the maximum halo current was more than one. The upper bound of the maximum halo current was determined by the discharges with the burst at $q_s \sim 1$, which suggests that the $q \sim 1$ magnetic surface is destroyed and a plasma current inside a plasma core is changed to the halo current rapidly.

A toroidal distribution sometimes showed an n = 1 structure with its peak position rotating with a rotation frequency of 500 ~ 700 Hz. Rotation frequency of the halo current correlated with the frequency of density and magnetic fluctuations. This may be caused by a kink type instability. At the timing of the maximum halo current, the rotation phase correlations between the magnitude of halo current and both fluctuations are not clear due to the burst at $q_s \sim 1$.

The temperature distribution during disruption was measured by YAG Thomson scattering system [2] with a repetition time of 50 ms. The central and edge electron temperatures before the energy quench were 1 - 1.8 keV and 200 - 400 eV respectively for the initial plasma current of 0.7 MA (Fig. 3). After the energy quench, T_e near the edge drops to 20 - 50 eV with a flat temperature profile.

T_e near the last flux surface gradually decreases during I_p-quench and reaches to 10 eV at 1 ms before the time of maximum halo current. In the case of $I_p = 1.2$ MA, the central electron temperature of 1.5 - 2.0 keV before the energy quench also drops to 10 eV.

2.2 Halo current data base

A halo current data base for the amplitude and toroidal peaking factor (TPF = maximum/average amplitude of the toroidal direction) was constructed by scanning the plasma parameters just before the disruption in the ranges of $I_p = 0.7 \sim 1.8$ MA, $B_T = 2.2 \sim 3.5$ T, $\kappa = 1.3 \sim 1.6$ and $q_{95} = 2.8 \sim 7.0$, respectively. Ranges of the measured total halo current normalized by initial plasma current (I_h/I_{p0}) and TPF were $0.05 \sim 0.26$ and $1.4 \sim 3.6$, respectively (see Fig. 4). The maximum TPF$^*I_h/I_{p0}$, corresponding to the maximum local halo current, was 0.52 so far, which was lower than that of the maximum value of the ITER data base of 0.75, and was also smaller compared with the present design value of ITER divertor cassette of 0.58. For NB heated discharges with the stored energy ($W_{dia}^{e\cdot q\cdot}$)of more than 1 MJ just before the energy quench, including three reversed magnetic shear discharges and one high β_p discharge, the maximum value of TPF$^*I_h/I_{p0}$ is about one third of the value of upper boundary (squares in Fig. 4). Significant reduction of TPF$^*I_h/I_{p0}$ was also observed for an intense neon gas puffing during VDE (closed circles in Fig. 4).

3. PARAMETER DEPENDENCIES

The upper boundary of TPF$^*I_h/I_{p0}$ tended to decrease with the increase in I_{p0}. No B_T dependence was observed. Other parameter dependencies of TPF$^*I_h/I_{p0}$ on κ and q_{95} were not clear. The driving forces of the halo current are considered to be an electric field generated by the decrease in toroidal and poloidal magnetic fluxes in a plasma caused by the vertical shift ($-dZ_j/dt$) and the plasma current decay ($-dI_p/dt$). Since the magnitude of the halo current is considered to be determined by the induced electric field and the resistance in the halo plasma, the effects of the driving forces and the resistance have been verified. We confirmed that the upper boundary of TPF$^*I_h/I_{p0}$ decreased with the decrease in $-dZ_j/dt$. On the other hand, the TPF$^*I_h/I_{p0}$ clearly decreases with the increase in $W_{dia}^{e\cdot q\cdot}$ (Fig. 5). This dependence is consistent with the dependence of the upper boundary of TPF$^*I_h/I_{p0}$ on the plasma current. TPF$^*I_h/I_{p0}$ clearly decreases with the increase in the line integrated electron density at the peak of the halo current as shown in Fig. 6.

These stored energy and density dependencies of the halo current is explained as following. When the released plasma energy at the energy quench increases with $W_{dia}^{e\cdot q\cdot}$, a large amount of impurity is generated at the divertor plates due to a large heat load. After that, the electron density increases and the electron temperature decreases in the halo plasma (the resistivity increases), then the halo current decreases. While a dependence of the electron temperature near the edge at the maximum halo current on the stored energy is not clear due to diagnostic errors, these experiment results support the possible mechanism where the magnitude of halo current is small for the low electron temperature at the halo plasma region.

4. REDUCTION AND AVOIDANCE OF HALO CURRENT

Based on the above results, reduction and avoidance methods of the halo current have been investigated. For reducing the temperature of the halo plasma, an intense pulse gas puff has been attempted. When hydrogen gas of 50 Pam^3/s x 0.1s was applied during VDE, the magnitude of the halo current decreased by about 40 %. In case of neon gas puff with the puffing rate and duration of 3.3 Pam^3/s x 0.17 s, the halo current reduced to 60 % of those of no gas puff case (Fig. 7). TPF$^*I_h/I_{p0}$ was always lower than 0.12 in this case. Thus, the neon puff is more effective to reduce the halo current. Electron temperature decreases form edge to center during neon puff, and the edge temperature drops to below 10 eV before the time of the maximum halo current (Fig. 8). The electron temperature at the timing of the maximum halo current can be expected to be lower than that for no gas puffing.

Furthermore, perfect avoidance of the halo current has been demonstrated by maintaining the plasma vertical position during the current termination. R. Yoshino et al [3] found that there is a vertical position where VDE is not observed during the I_p-quench. In this point (neutral point), the total vertical force was almost zero due to an optimal distribution of the vacuum vessel eddy currents. In JT-60U, the neutral point is $Z_j = +15$ cm because of an up-down asymmetry of the vacuum vessel

and PFC. Simulations by the Tokamak Simulation Code (TSC) confirmed the experimental observation of the zero VDE growth rate at the neutral point [4].

We conclude that the magnitude of the halo current during high performance discharges is expected to be small compared to that in the OH case from the parameter dependencies studies. For OH discharges only, a large plasma current should result in a small I_h/I_{p0} because of the large $W_{dia}^{e \cdot q}$. This result has an advantage for the next generation tokamaks with high performances and a large plasma current. The neon gas puffing is effective to reduce the halo current.

REFERENCES

[1] WESLEY, J., et al., in Plasma Physics and Controlled Nuclear Fusion Research 1996 (Proc. 16th Int. Conf. Montreal, 1996), Vol.2, IAEA, Vienna (1997) 971.
[2] HATAE, T., et al., will be published in Rev. Sci. Instrum. "YAG laser Thomson scattering diagnostics on the JT-60U"
[3] YOSHINO, R., NAKAMURA, Y., NEYATANI, Y., Nucl. Fusion 36 (1996) 295.
[4] NAKAMURA, Y., YOSHINO, R., NEYATANI, Y., TSUNEMATSU, T., AZUMI, M., Nucl. Fusion, 36 (1996) 643.
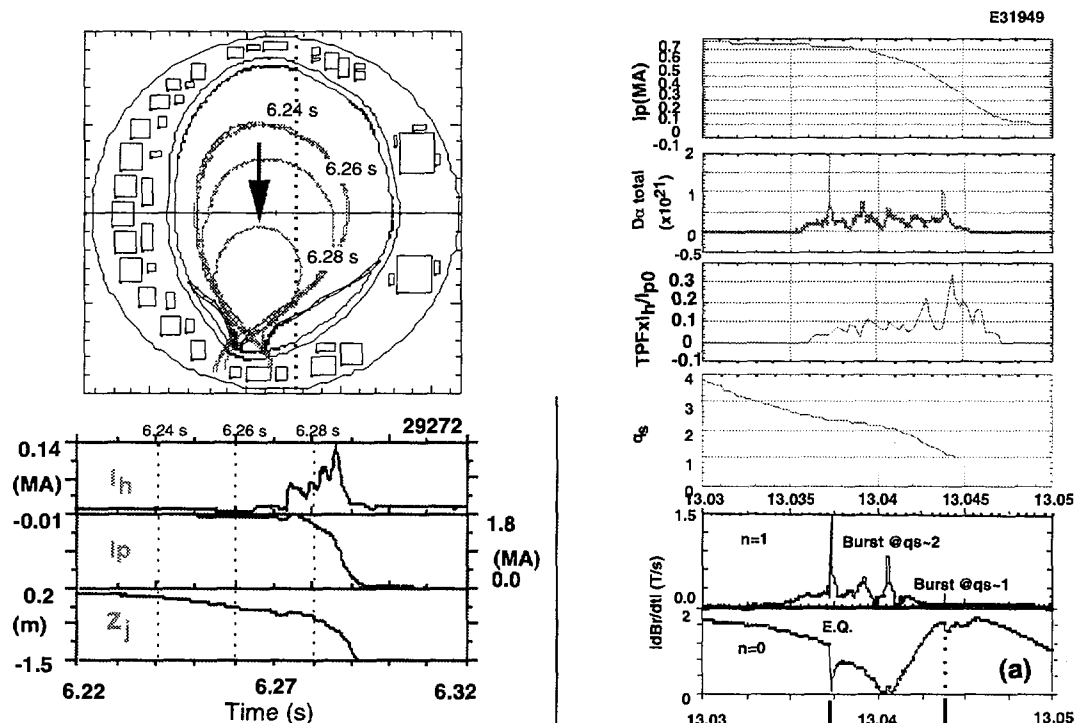
Fig. 1. Waveforms of the halo current during a simulated VDE. A plasma is shifted downward actively to simulate VDE. The dotted line in the upper figure indicates the line of sight of FIR measurement. Halo current starts to flow from t = 6.265 s and reaches its maximum at t = 6.286 s.

Fig. 2. Three |dBr/dt| bursts with Dα bursts at the energy quench (13.037s), q_s~2 (13.04 1s) and q_s~1 (13.043s) occurs during simulated VDE. |dBr/dt| is measured by saddle loops located at outer midplane. Slow change of n=1 component corrensponds to downward motion of the plasma.
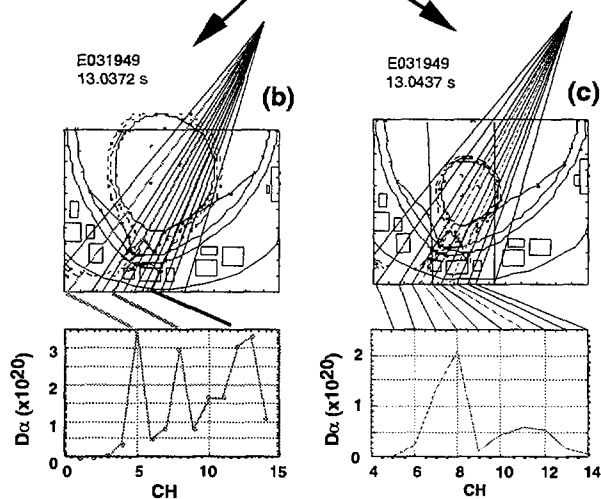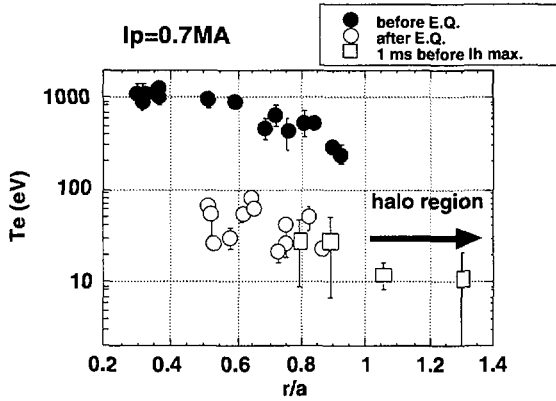
Fig. 3. Distribution of the electron temperature at three time slices. Three time slices are obtained from three discharges.
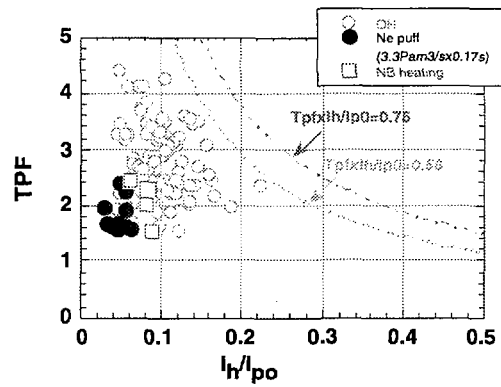

Fig. 4. Toroidal Peaking Factor (TPF) versus normalized halo current defined by I_h/I_{p0}. Where I_{p0} is a plasma curren just before the current quench.
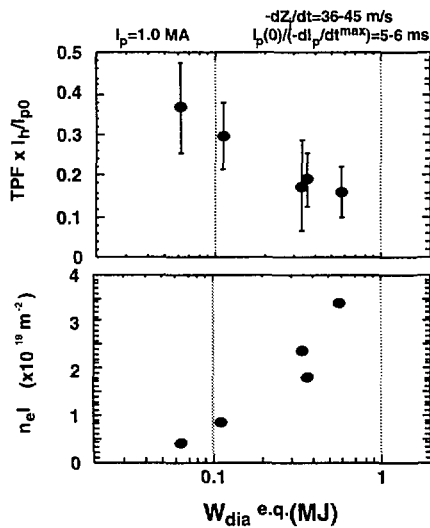

Fig. 5. Relation between $TPF \times I_h/I_{p0}$, $n_e l$ and the stored energy just before the energy quench ($W_{dia}^{e.q.}$). The stored energy is varied by changing the NB heating power for a fixed plasma current of 1 MA.

Fig. 7. Wave forms of halo current with (3.3 Pam^3/s x 0.17 s) and without neon gas puffing.

Fig. 6. The $TPF \times I_h/I_{p0}$ versus line integrated electron density ($n_e l$) at the time of the maximum halo current for a vertical shift velocity ($-dZj/dt$) of 36-45 m/s.
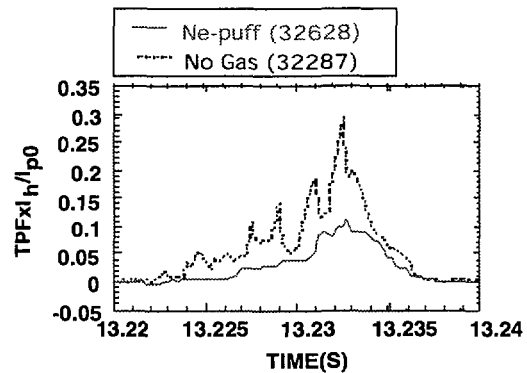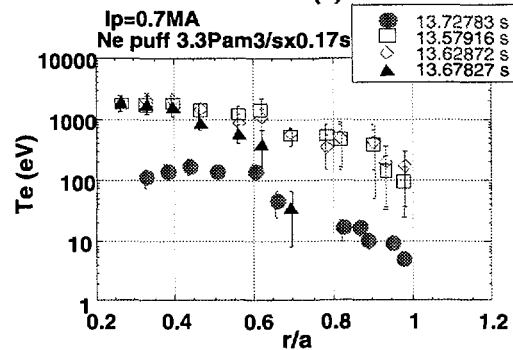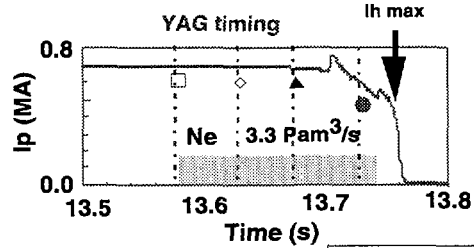

Fig.8. Distribution of the electron temperature measuerd by YAG Thomson scattering at every 50 ms during neon puffing discharge.